Biogeosciences, 8, 2567–2579, 2011
www.biogeosciences.net/8/2567/2011/
doi:10.5194/bg-8-2567-2011

Biogeosciences

Exploring B/Ca as a pH proxy in bivalves: relationships between *Mytilus californianus* B/Ca and environmental data from the northeast Pacific

S. J. McCoy[1], L. F. Robinson[2,3], C. A. Pfister[1], J. T. Wootton[1], and N. Shimizu[2]

[1]Department of Ecology and Evolution, University of Chicago, Chicago, IL 60637, USA
[2]Department of Marine Chemistry and Geochemistry, Woods Hole Oceanographic Institution, Woods Hole, MA 02543, USA
[3]Department of Earth Sciences, University of Bristol, Bristol BS8 1RJ, UK

Received: 29 May 2011 – Published in Biogeosciences Discuss.: 9 June 2011
Revised: 2 September 2011 – Accepted: 7 September 2011 – Published: 13 September 2011

Abstract. A distinct gap in our ability to understand changes in coastal biology that may be associated with recent ocean acidification is the paucity of directly measured ocean environmental parameters at coastal sites in recent decades. Thus, many researchers have turned to sclerochronological reconstructions of water chemistry to document the historical seawater environment. In this study, we explore the relationships between B/Ca and pH to test the feasibility of B/Ca measured on the ion probe as a pH proxy in the California mussel, *Mytilus californianus*. Heterogeneity in a range of ion microprobe standards is assessed, leading to reproducible B/Ca ratios at the 5 % level. The B/Ca data exhibit large excursions during winter months, which are particularly pronounced during the severe winters of 2004–2005 and 2005–2006. Furthermore, B/Ca ratios are offset in different parts of the skeleton that calcified at the same time. We compare the *M. californianus* B/Ca record to directly measured environmental data during mussel growth from the period of 1999–2009 to examine whether seawater chemistry or temperature plays a role in controlling shell B/Ca. A suite of growth rate models based on measured temperature are compared to the B/Ca data to optimise the potential fit of B/Ca to pH. Despite sampling conditions that were well-suited to testing a pH control on B/Ca, including a close proximity to an environmental record, a distinct change in pH at the sampling locale, and a growth model designed to optimise the correlations between seawater pH and shell B/Ca, we do not see a strong correlations between pH and shell B/Ca (maximum coefficient of determination, r^2, of 0.207). Instead, our data indicate a strong biological control on B/Ca as observed in some other carbonate-forming organisms.

Correspondence to: S. J. McCoy
(mccoy@uchicago.edu)

1 Introduction

The accretionary skeletons of modern and fossil organisms can provide valuable archival information about past environmental conditions and climate. For example, growth data can serve as an indicator of growth conditions, as organisms tend to grow faster at species-specific optimal conditions (Schöne et al., 2005). Furthermore, chemical impurities incorporated in skeletal tissue, including trace metals and stable isotopes, can be used to reconstruct an organism's growth environment as a time series over its lifetime. Such sclerochronological data are commonly used in the geosciences to reconstruct past environments where no instrumental data exist.

Reconstruction of ocean chemistry, particularly pH, has become increasingly important as the marine scientific community focuses attention on climate change. Continued release of CO_2 to the atmosphere and subsequent uptake by the ocean may lead to abrupt changes in ocean pH and carbon chemistry, more rapid than any change during the past 300 million years (Caldeira and Wickett, 2003). The responses of nearshore organisms to ocean acidification therefore could be a pervasive and critical problem for marine ecosystems, and it is therefore important to assess the extent of recent ocean acidification in the nearshore environment.

Incorporation of trace metals into the carbonate skeletons of marine organisms depends on the combined effects of biological controls (vital effects) and environmental parameters such as temperature, pH and salinity (Lutz, 1981; Takesue and van Geen, 2004; Weiner and Dove, 2003). In particular, pH has been shown to affect the relative abundance of boron (B) in the shells of calcifying organisms (Hemming and Hanson, 1992; Yu and Elderfield, 2007). Dissolved B is found predominantly as boric acid ($B(OH)_3$) or borate ($B(OH)_4^-$) in seawater, and the relative abundances of these species

are pH-dependent (Hemming and Hanson, 1992). Borate is thought to be the primary chemical species incorporated into carbonates following Eq. (1) (Hemming and Hanson, 1992).

$$CaCO_{3(aq)} + B(OH)^-_{4(aq)} \rightleftharpoons \quad (1)$$

$$Ca(HBO_3)_{(s)} + HCO^-_{3(aq)} + H_2O$$

The partition coefficient, K_D, can be obtained from Eq. (1), yielding:

$$K_D = \frac{[HBO_3^{2-}]/[CO_3^{2-}]_{(CaCO_3)}}{[B(OH)_4^-/HCO_3^-]_{(seawater)}} = \frac{[B/Ca]_{(CaCO_3)}}{[B(OH)_4^-]/[HCO_3^-]_{(seawater)}} \quad (2)$$

$$[B/Ca]_{(CaCO_3)} = K_D \cdot [B(OH)_4^-/HCO_3^-]_{(seawater)} \quad (3)$$

Recent work has revealed that both BO_3 and BO_4 groups have been found in both biogenic aragonite and calcite (Klochko et al., 2009; Rollion-Bard et al., 2011a; Sen et al., 1994), although it remains unclear whether the BO_3 species found in the crystal originates from boric acid in seawater or from a coordination change of the borate ion (Klochko et al., 2009; Sen et al., 1994).

The residence time of Ca in the ocean is 1.1 million years (myr) (Broecker and Peng, 1982) and that of B is estimated between 14 and 20 myr (Pagani et al., 2005; Spivack and Edmond, 1987; Lemarchand et al., 2000). Thus, the total concentration of B in the modern ocean is constant over the timescales relevant to this study at around 4.52 ppm in open marine environments (Lee et al., 2010). While total B, Ca and C concentrations remain constant (Lemarchand et al., 2000; Kennish, 1989), the ratio of $[B(OH)_4^-]/[HCO_3^-]$ (mol/mol) in the modern ocean is proportional to pH, as increasing pH both increases borate and decreases bicarbonate ion concentrations (Yu et al., 2007).

Although the relationship between pH and boron isotopic ratio ($\delta^{11}B$) has been explored in a number of species (Foster, 2008; Hemming and Hanson, 1992; Hönisch et al., 2007; Hönisch and Hemming, 2005; Sanyal et al., 2000; Yu et al., 2007) and the general pH-dependence of B/Ca and $\delta^{11}B$ are understood, species-specific relationships between B/Ca and pH as well as B/Ca and $\delta^{11}B$ remain unclear. Recent studies using planktonic foraminifera have suggested species-specific relationships between B/Ca (µmol/mol) and seawater $[B(OH)_4^-]/[HCO_3^-]$, based on differences in the relationship between K_D and both temperature and $[CO_2]$ (Foster, 2008; Yu et al., 2007). Besides planktonic foraminifera and single samples of each of several aragonitic coral species and abiogenic ooids, only one sample each of a calcitic brachiopod, a high-Mg calcite red coralline alga, and an aragonitic calcareous green alga have been analysed for B concentrations and $\delta^{11}B$ (Hemming and Hanson, 1992). Thus, B abundance over a range of pH within one species has been measured only in inorganic precipitates and planktonic foraminifera over large-scale pH differences (Foster, 2008; Hemming and Hanson, 1992).

Many sclerochronological studies have used the fossil or modern shells of marine bivalves (Dodd, 1964; Goodwin et al., 2001; Killingley and Berger, 1979; Klein et al., 1996; Lutz, 1981; Schöne et al., 2005). However, analysis of large samples with accretionary shells introduces the problem of reconstructing the growth chronology of an organism that may be secreting its shell seasonally or discontinuously. Without detailed field studies of how growth rates change within the season, determination of an absolute chronology on a sub-annual timescale can be difficult. For this reason, most studies using bivalves focus on overall trends in shell chemistry rather than absolute timescales (Blamart et al., 2007; Foster et al., 2008; Klein et al., 1996; Lutz, 1981). One way to address this problem is to couple measured environmental parameters with changes in shell chemistry made at a sufficiently high resolution.

In this study, we take advantage of a 9-year instrumental record of ocean environmental variables including pH and temperature (Pfister et al., 2007; Wootton et al., 2008) and use it to address the difficulties of correlating sclerochronological data from an organism with an uncertain growth history, sampled at a different frequency than available environmental data. We measure B concentration by ion microprobe in the shell of the California mussel, *Mytilus californianus*, and compare the relationship between measured B/Ca and an instrumental record of pH and temperature at the mussel's growth site, Tatoosh Island, Washington (Pfister et al., 2007; Wootton et al., 2008). We use growth rates and environmental data to determine the growth chronology of *M. californianus* and discuss the various controls on B incorporation into the shell. By reconstructing ocean chemistry through sclerochronological changes in mussel shell chemistry, we document biologically relevant changes in seawater chemistry recorded in the mussel's growth environment while addressing the issue of concatenating growth patterns with high-resolution environmental records.

B/Ca in marine carbonates is typically measured by inductively coupled plasma-mass spectrometry (ICP-MS). However, B can be difficult to measure by ICP-MS, due to (1) spectral overlap of the ^{12}C peak on the ^{11}B peak, (2) nebulisation of acidic solutions resulting in high B blank values from the entrance system, and (3) high B concentrations in the sample that may cause memory effects (Al-Ammar et al., 1999, 2000; Sah and Brown, 1997; Yu et al., 2007). In addition to these technical complexities, preparation of carbonate samples for ICP-MS is time-consuming and meticulous. Carbonate samples must be drilled from the mussel shell and dissolved in a nitric acid solution and sampling resolution is limited by drilling precision and drill size. We chose the ion microprobe for its high-resolution sampling along the shell surface and high measurement precision (Shimuzu and Hart, 1982). We tested a range of organic and inorganic carbonate standards for calibration, and discuss method development

for reproducible boron concentration measurement by ion microprobe.

2 Samples and methods

2.1 *Mytilus californianus*

M. californianus, the California mussel, is an intertidal mussel living on the Pacific coast of North America. At Tatoosh Island, WA (48.4° N, 124.7° W), the 1997/1998 El Niño disturbance enabled *M. californianus* to invade via establishment of new recruits in 1999 (Paine and Trimble, 2004). Our specimen was collected live at Tatoosh Island on 17 April 2009. Thus, we know the year of first growth as well as the exact time of collection for this sample, enabling us to identify yearly growth banding within the shell. Visible annual banding matches the expected time from recruitment to collection. Furthermore, a Hydrolab DataSonde multi-probe (Hach Company, Loveland, Colorado, USA) was deployed adjacent (∼10 m) to these mussel beds at approximately the same tidal depth in June 2000 (Pfister et al., 2007; Wootton et al., 2008). The coincidence of environmental data and well-dated sample provides an excellent opportunity to test the incorporation of traces metals into bivalve shells in a dynamic environment. In this study, we analysed the left valve of one shell, measuring 156.3 mm in length, 61.2 mm in width, and 58.2 in height (both valves) (Fig. 1).

2.2 Sample chronology

M. californianus consists of a thick, yearly-banded inner layer of prismatic calcite, a very thin nacreous aragonite layer, an outer layer of tidally banded prismatic calcite, and a coating of organic matter called the periostracum (Fig. 1) (Dodd, 1964). The calcitic inner prismatic layer is present only in *M. californianus*, and not in any of its closely related species (Dodd, 1964). The beak region is the extension of the inner prismatic layer into the apex of the shell hinge, and is often discoloured due to higher concentrations of organic matter within the $CaCO_3$ matrix (Takesue et al., 2008). The inner prismatic layer accretes inward whereas the outer prismatic layer accretes outward (Fig. 1).

While specific patterns of shell deposition have not been documented for *M. californianus*, useful inferences can be made from known patterns of accretion in other bivalves such as *Geukensia demissa*, *Mercenaria mercenaria*, and *Pinctada radiata* (Lutz and Rhoads, 1977). The pattern of light and dark growth bands in bivalve shells come from the alternation of shell deposition during aerobic respiration and dissolution during periods of anaerobic respiration when the shell is closed, such as during low tide. During aerobic respiration, calcification creates thick bands of calcite. During a period of anaerobic respiration, the acidic end products of anaerobic metabolism are neutralised by the dissolution of calcite from the shell, leaving behind a relatively

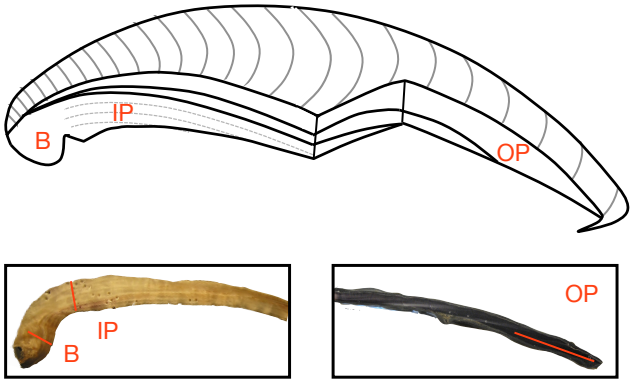

Fig. 1. A cross-sectional sketch of *M. californianus*, modified from Dodd (1964). Shell regions are labelled (B, beak; IP, inner prismatic; OP, outer prismatic) in red. Sample transects are shown in red on the shell photographs above.

insoluble residue that is rich in organic matter at the interface of the mantle and the most recently deposited shell layer (Lutz and Rhoads, 1977). At the microstructural level, tidal cycles can be resolved in the outer shell layer as bivalves respire anaerobically during low tides. Thick bands of calcite are deposited during the growth season, making the annual cycle more obvious. When water temperatures are coldest and oxygen transport within the animal is most reduced, shell dissolution may dominate over shell growth (Lutz and Rhoads, 1977). Dissolution compounded with a decrease in growth rate with declining temperature creates very thin, dark organic-rich winter growth bands compared to thick summer growth bands.

Sample years in our specimen were assigned using seasonal banding patterns visible in the shell cross-section, and counting back from the known last full growth season, 2008. We were able to assign yearly chronology to the growth bands, and year assignments were confirmed by the fact that the number of growth layers in the shell was consistent with our known start and end dates of mussel growth. Samples analysed in the inner prismatic layer span 1999–2008, and those from the beak region and outer prismatic layer span 2004–2008.

Because the specific within-season pattern of growth is unknown in *M. californianus*, we modeled growth within the year both as a constant and also as a seasonal function of temperature. Thus, linear and sinusoidal within-year growth chronologies were both explored, corresponding with constant and temperature-dependent growth, respectively. Environmentally-dependent growth has been suggested in bivalves, particularly for *Mytilus* species (Coe, 1965; Lutz and Rhoads, 1977; Malone and Dodd, 1967). Within each model, band fraction was assigned as a function of the fraction of the length between the previous winter band and the sample spot over the total thickness of the growth band, leaving out those samples that fell directly on dark winter banding. In both

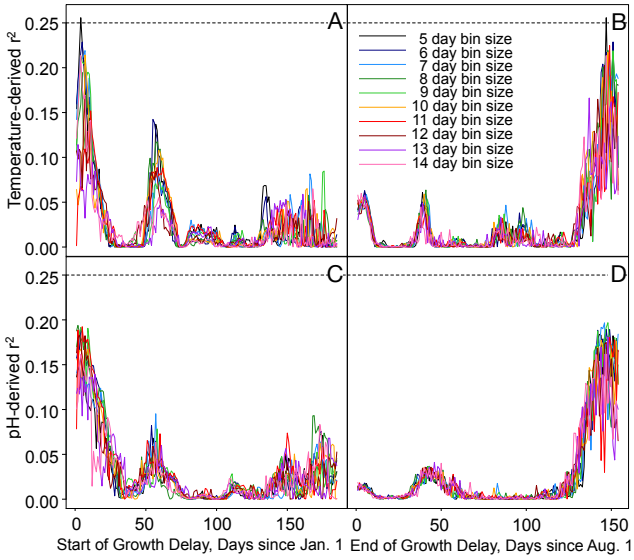

Fig. 2. Coefficients of variation (r^2) for sinusoidal growth models. Panels shows r^2 between B concentration (ppm) and water temperature (**A**, **B**) and pH (**C**, **D**) based on growing season lag times for onset of the growing season (**A**, **C**) and termination of the growing season (**B**, **D**). Each color represents a different bin size for environmental data: 5 days, black; 6 days, navy blue; 7 days, blue; 8 days, dark green; 9 days, light green; 10 days, orange; 11 days, red; 12 days, dark red; 13 days, purple; 14 days, pink.

the linear and sinusoidal chronologies, we varied the length of the growing season by starting growth between 1 January and 30 June, and ending growth between 1 August and 31 December. This was meant to simulate a period of slow or nonexistent growth that has been documented in bivalves during winter months, referred to here as the lag period (Coe, 1965; Malone and Dodd, 1967).

Without additional information, we would not be able to asses which of these models were correct. In order to provide additional insights we compared our B/Ca data to each growth rate model comparing the two parameters (temperature and pH), which have been shown to affect B/Ca in foraminifera. We also compared model fits to atmospheric CO_2, chlorophyll-*a*, estimated alkalinity, salinity, daily upwelling index, and PDO index, all of which fit very poorly in comparison to temperature and pH and are thus not discussed here. Despite this approach, our final conclusions on the controls on B/Ca are not dependent on the fit because we do not find a strong correlation. Because of our sampling resolution (50 µm spot size within a growth band typically ∼3000 µm wide), we assumed that each data point represents a time-averaged environment. To allow direct comparison between analytical and environmental data, all environmental data was first averaged to a daily scale and subsequently analysed using a rolling mean with varying bin sizes of 5–28 days. Such a large range in bin size was used to explore the full range of possibilities in growth rate. Next, binned pH and temperature measurements were compared to each linear and sinusoidal model over all lag periods. To do so, each growth model was used to assign sample chronology to the B/Ca data, and then B/Ca was compared to binned environmental data at corresponding dates. The best-fit models for pH and temperature were selected using coefficients of determination (r^2 values). We define the best-fit model as having the highest coefficient of determination, which is indicative of how well the model correlates with the data (Fig. 2). We changed the lag period by optimising both start and end dates of the lag period (Fig. 2). Lag periods in bivalves may be related to low-temperature thresholds (Coe, 1965; Malone and Dodd, 1967).

2.3 Sample preparation

All soft parts of the shells were immediately removed at time of collection and shells were dried in an oven at 40 °C. Shells were scrubbed in a 5 % bleach solution and soaked for 1 h, then rinsed 3 times in MilliQ water for 15 min (Schöne et al., 2006). Specimens were mounted on Lexan cubes and coated in JB Kwik Weld (JB Weld Co., Sulphur Springs, TX, USA) metal epoxy. Two mirror cross sections (1.5 mm) were cut along the axis of maximum growth using a Buehler Diamond Wafering Blade (0.4 mm, Buehler Co., Lake Bluff, IL, USA) on an Isomet saw. In preparation for analysis by ion microprobe, the areas of interest were cut from the sample cross section using a dremel tool, polished on 800 grit followed 1200 grit silicon carbide paper (Buehler Co.) and subsequently polished with a 0.3 µm diamond suspension (MetaDi Polycrystalline Diamond Suspension, Buehler Co.) on a felt surface. The samples were then mounted in indium, rinsed with MilliQ water and placed in a drying oven at 50 °C. The sample mounts were gold-coated via sputtering and stored in a vacuum oven prior to analysis.

2.4 Ion microprobe SIMS analysis

Ion microprobe analysis was conducted over 5 days on a CAMECA IMS 1280 (Northeast National Ion Microprobe Facility, Woods Hole, MA) using a caesium (Cs^+) ion beam analysed with secondary ion mass spectrometry (SIMS). Analysis was conducted following Shimizu and Hart (1982) and Hart and Cohen (1996). The primary ion beam used was $^{133}Cs^+$, typically 5–6 nA, rastered over 30 by 30 µm. We measured the secondary ions $^{11}B^-$ and $^{40}Ca^-$ with a mass resolving power (MRP) of 3100 to separate ^{40}Ca from $^{24}Mg^{16}O$. A field aperture of 15 by 15 µm was placed at the centre of the rastered area, giving an effective central analysis area of 15 by 15 µm. Our count rates were, on average, approximately 250 cps (counts per second) and 50 000 cps for $^{11}B^-$ and $^{40}Ca^-$, respectively. $^{11}B/^{40}Ca$ ratios measured for 10 cycles had a 1-sigma standard error of 0.6 %. The B signal is sensitive to surface contamination, so sample spots were pre-cleaned using a pre-sputtered routine for 120 s prior to

Table 1. List of standards and their absolute B concentrations.

Standard name	Composition	[B] (ppm)
carr 1	Carrara biogenic marble	0.306
carr 2	Carrara biogenic marble	0.306
carr 3	Carrara biogenic marble	0.306
oka1	Canadian carbonatite	0.68
oka2	Canadian carbonatite	0.68
odp209	low-T inorganic aragonite vein	15.6
0875	inorganic calicte	29.2
ber007	aragonitic coral	67

measuring $^{11}B^-$ and $^{40}Ca^-$ to remove the gold coating and surface contaminants. Sputtering time for each block of data collection was 120 s, and data was collected over 5 blocks (total 600 s per sample spot).

Standardisation when making accurate concentration analyses by in situ methods has been a long-standing challenge. Ion probe analyses on carbonates are particularly challenging because most natural carbonates are heterogeneous and the spot size is small. Typically, ion probe data are normalised using a suite of known-concentration standards to derive an empirical working calibration curve for each day's analyses. In this study, we used five carbonate standards that have been previously been used for trace metal analyses in corals and that were mounted and polished in the same way as the *M. californianus* samples (Hart and Cohen, 1996; Stoll et al., 2007). The standards include a Carrara biogenic marble crystal (carr1, carr2, carr3: 0.306 ppm B), a Canadian carbonatite crystal (oka1, oka2: 0.68 ppm B), a low-temperature inorganic aragonite vein (odp209: 15.6 ppm B), an inorganic calcite crystal (0875: 29.2 ppm B), and an aragonitic coral (ber007: 67 ppm B) (Fig. 4, Table 1). The bulk boron concentration of each one has been determined by solution ICP-MS, which homogenises a portion of the crystal that is larger than that sampled by ablation. Thus, solution ICP-MS measurement provides an average value for the crystal. In order to achieve an accurate B concentration by ion microprobe on each standard, we deliberately measured standards over the entirety of the crystal, leading to low precision but high accuracy. Initial analyses demonstrated that the standards were not as homogeneous as had been anticipated, requiring significant effort to be focused on mapping and characterising the standards to produce consistent results (Fig. 3).

The two aragonite standards odp209 and ber007 were particularly heterogeneous with standard deviations of up to 15 ppm B (79 %) in odp209 on only one day (Figs. 3, 4). Repeated analyses on different days suggest that the standard has distinct areas of high and low B concentration (Fig. 3). Given it's formation environment, it is not surprising that the coral standard (ber007) showed large variations of up to 11 ppm B (19 %) within one day, and again seemed to be clustered into areas of low and high B concentration. We chose not to use these two highly heterogeneous standards in our daily working curves. The standard reproducibility within carr and oka were within 1 ppm B compared both within and among days, and 0875 varied under 2.5 ppm overall. There are two approaches to using these crystals as standards: (a) perform repeated analyses that cover the whole crystal to get a representative concentration each day, or (b) focus on a small area to get the most precise number. The former will give the most accurate concentration with low precision, and the latter would give higher precision with low accuracy. For this study we utilised the standardisation scheme most likely to improve accuracy from day to day, i.e. we spread analyses across the entire standard crystal to get the most representative B concentration. By following this approach we found that replicate analyses on adjacent samples on the *M. californianus* sample section are within 3 % when measured on the same day and 5 % when measured on different days. We also followed this procedure to account for instrument drift over the day. Given that B concentration ranges over 1–60 ppm among study samples, this level of reproducibility is more than adequate for the aims of the study. This result demonstrates that heterogeneity exists in the standards, but that the ion microprobe can give accurate and relatively precise data for this type of sample given careful calibration.

Calcitic layers from three distinct regions of *M. californianus* were sampled for B/Ca (Fig. 1). Sampling resolution was determined by thickness of each individual growth layer in each shell region, and therefore the temporal resolution varies by year and shell layer. The inner prismatic layer was sampled by 83 consecutive samples of 50 µm spot size over ten years of growth, with a resolution of one sample every 2–3 weeks from 1999–2008, and one sample every 1–2 weeks in 2005. The beak region is sampled by 34 consecutive samples over five years of growth from 2004–2008 at approximately one sample per month. The outer prismatic layer is sampled by four overlapping transects with a total of 75 samples over five years of growth, averaging one sample per month during 2004, 2005, and 2008, and one sample per week during 2006 and 2007.

2.5 Environmental and hydrographic data

Chlorophyll-*a*, pH, salinity, and temperature were all measured directly every 30 min at the site of collection with a Hydrolab DataSonde multi-probe (Hach Company, Loveland, Colorado, USA) on Tatoosh Island, WA from April–September each year since 2000. The precise location of the Hydrolab DataSonde was ∼10 m from the collection site of our shell sample. The Hydrolab environmental dataset was filtered to remove datapoints taken at low tide (Wootton et al., 2008), and the instrument was deployed at approximately the same tidal height as the growth environment of our *M. californianus* specimen. The pH probe used a 3M KCl solution with saturated AgCl as the reference cell electrolyte,

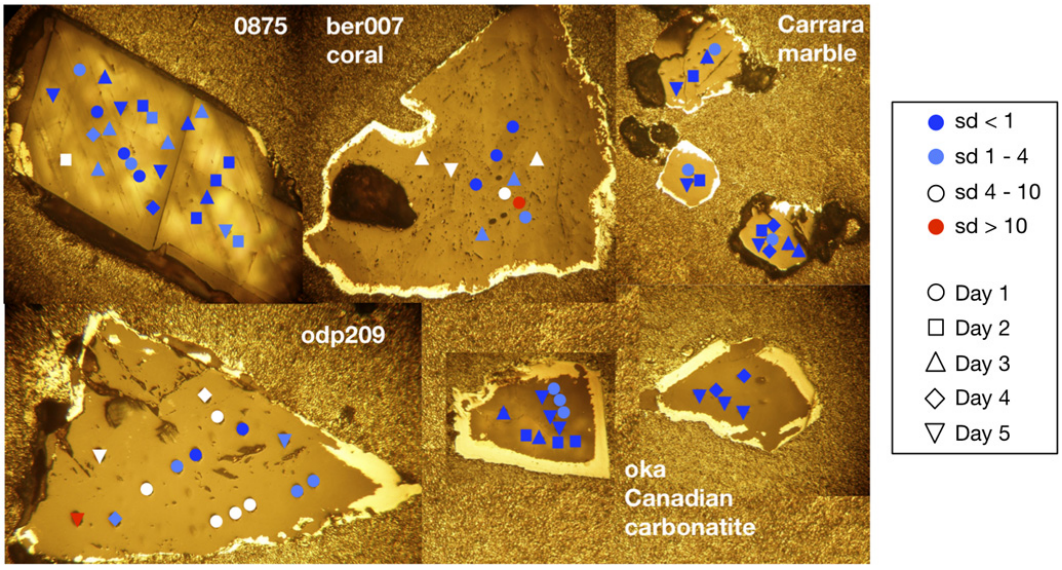

Fig. 3. Standard heterogeneity index. Point color represents the standard deviation between the B concentration (ppm) of the point measured on that day and converted using that day's calibration curve and the absolute value of the standard. Standard deviation (sd) < 1 is represented by dark blue, sd 1–4 by light blue, sd 4–10 by white, and sd ≥ 10 by red (i.e. high proportion of blue points indicates a good quality standard with low heterogeneity). The shape of the point refers to the measurement day: Day 1, circle; Day 2, square; Day 3, triangle point up; Day 4, diamond; and Day 5, triangle point down.

and was calibrated with pH 7 and 10 NBS standards approximately every 2 weeks. Drift in pH measurements was accounted for by development of a non-linear statistical relationship between pH and time since service, and subtracting this relationship from the data (see methods of Wootton et al., 2008, for additional information). Summer surface water temperatures at Tatoosh Island range 8–12 °C (Pfister et al., 2007). pH exhibits a diurnal cycle spanning 0.24 units on average, largely driven by photosynthesis and respiration of large kelp beds at the study site (Wootton et al., 2008). Yearly average pH ranges between 7.78 and 8.41, with an overall decrease from 8.37 in 2000 to 7.79 in 2008. To more accurately compare environmental data to our *M. californianus* B/Ca dataset, we resampled the environmental dataset at lower temporal frequency using a rolling mean to match the frequency of B/Ca sampling. Both complete (30-min resolution) and resampled coastal environmental data show a distinct statistical trend in pH over time (Fig. 5) with no large or consistent fluctuations in either salinity or temperature, providing a unique opportunity to investigate pH control on *M. californianus* B/Ca.

Regional seawater ion concentration data from Global Ocean Data Analysis Project (GLODAP, Key et al., 2004) from 47.5° N, 124.5° W at 0 m depth near Tatoosh Island (48.4° N, 124.7° W) were used in addition to directly-measured data from Tatoosh Island to estimate total dissolved inorganic carbon (DIC), total alkalinity (ALK) and anthropogenic CO_2 in surface waters using the CO2sys Excel Macro (Pierrot et al., 2006). Daily upwelling and PDO indices were obtained from NOAA (National Marine Fisheries Service, http://www.pfeg.noaa.gov/).

3 Results

3.1 Analytical results

B concentration measurements at monthly resolution from the inner prismatic layer show strong seasonal signals with the highest values observed during winter bands (Fig. 6). Higher-frequency variation within each growing season is also apparent. Measurements from the summer growth season range from approximately 28–80 µmol/mol B/Ca, with a mean value of 45 µmol mol^{-1} from 1999 to 2008. Winter excursions in the inner prismatic layer reach up to 519 µmol mol^{-1} B/Ca in the winter of 2005–2006 and 187 µmol mol^{-1} in the winter of 2004–2005. Other winter bands in the inner prismatic layer did not show such pronounced high values. Measurements in the beak region show no winter excursions although sampling was continuous through the winter growth band. Summer growth season measurements range from 28–120 µmol mol^{-1} B/Ca, and average 66 µmol mol^{-1} from 2004 to 2008. As for the beak region, B/Ca in the outer prismatic layer shows no high values in winter samples. The B/Ca record from the outer prismatic layer ranges from 14–88 µmol mol^{-1} B/Ca, with a mean value of 39 µmol mol^{-1} from 2004 to 2008. Summer growth season measurements from the inner and outer prismatic layers show similar average values, although the outer

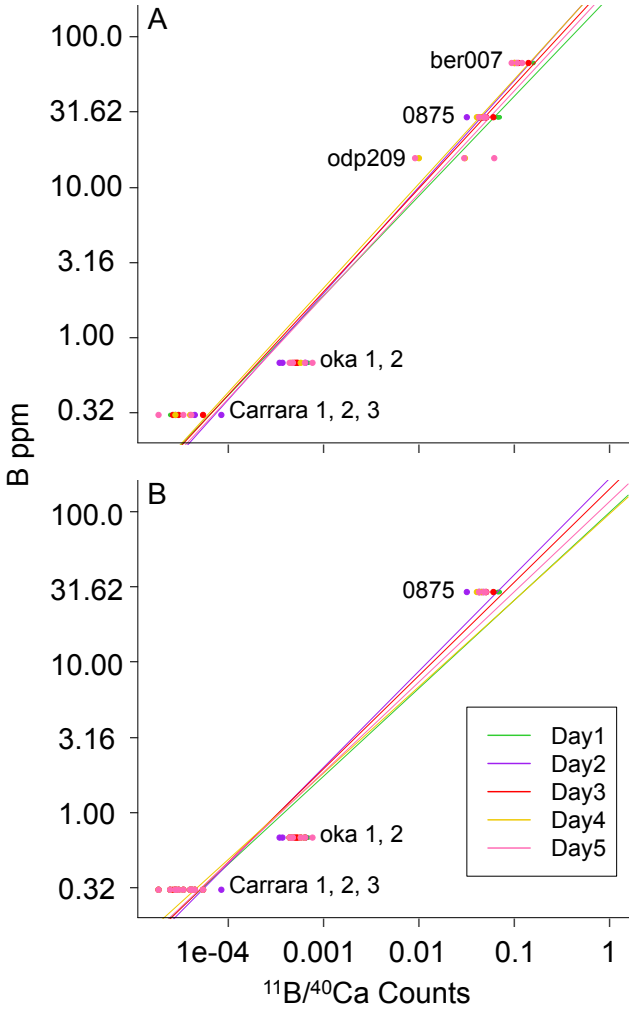

Fig. 4. Calibration curves shown on a $\log_{10}$ scale. **(A)** Calibration curve including all standards measured on all days. **(B)** Working calibration curve, excluding ber007 and odp209. In panels **(A)** and **(B)**: Day 1 shown in green; Day 2, purple; Day 3, red; Day 4, gold; and Day 5, pink.

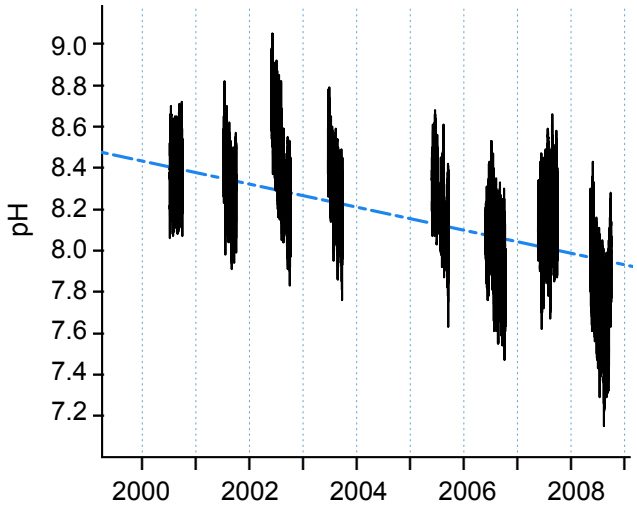

Fig. 5. Plot of pH data measured every 30 min from Tatoosh Island, WA (updated from Wootton et al., 2008). Dashed blue line shows statistically significant decline (highly significant, $p = 2.2e-16$).

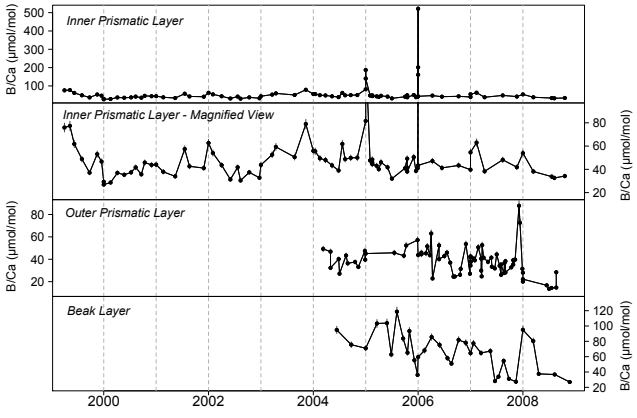

Fig. 6. Plots of complete ion probe B/Ca data from each shell layer, including measurements from winter bands. The locations of winter bands are indicated by vertical dashed shaded lines.

layer is sampled at higher temporal resolution. Our transect across the inner prismatic layer has the longest record and highest certainty of chronology due to better resolution of yearly banding in that layer. We thus use primarily the record from the inner prismatic layer to assess relationships between mussel shell B/Ca and environmental variables.

3.2 Growth chronology

The correlation of environmental data to shell B/Ca from the inner prismatic layer depended upon whether we assumed constant or seasonal (sinusoidal) growth patterns, with sinusoidal growth based on temperature as the best model. The maximum coefficients of determination were an order of magnitude higher in the sinusoidal models versus the linear, and the best-fit sinusoidal model was based on temperature, with an r^2 of 0.256 ($p = 0.0031$ using 5-day data bin; $r^2 = 0.192$, $p = 0.018$ for pH using 9-day data bin) (Fig. 7). This model fit with both temperature and pH was statistically significant, to the 0.001 level with temperature and 0.01 level with pH. As mentioned, the sinusoidal fit is consistent with a low-temperature threshold for winter growth (Coe, 1965; Malone and Dodd, 1967), as well as with the temperature-dependence of chemical substitution kinetics (Eq. 2). This best-fit model assumes that the mussel growth days were from 4–358 during the year (4 January–24 December, growing season length of 354 days). Overall, a bin size of 5–10 days provided the best fit, consistent with our 50 µm ion probe spot size analysing a time-averaged 1–2 weeks. When a larger data bin size was used, the coefficient of determination between shell B/Ca and both temperature and pH

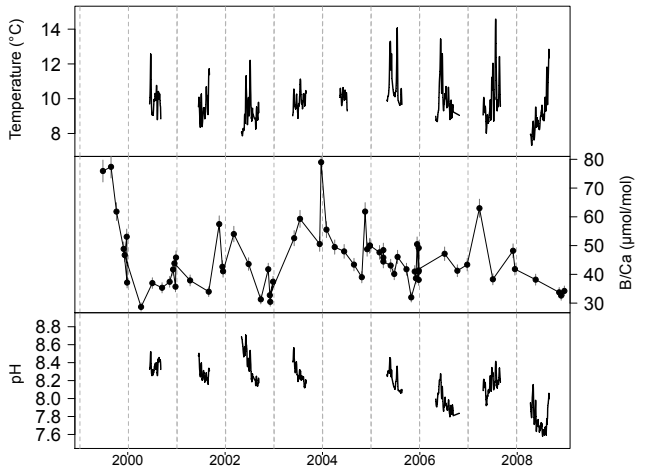

Fig. 7. Plots of pH, *M. californianus* B/Ca, and temperature. pH and Temperature shown here are binned at 5 days (according to best-fit model) and B/Ca chronology was obtained using the best-fit model. Dashed vertical lines represent a winter growth break, and year labels correspond to the start of that year.

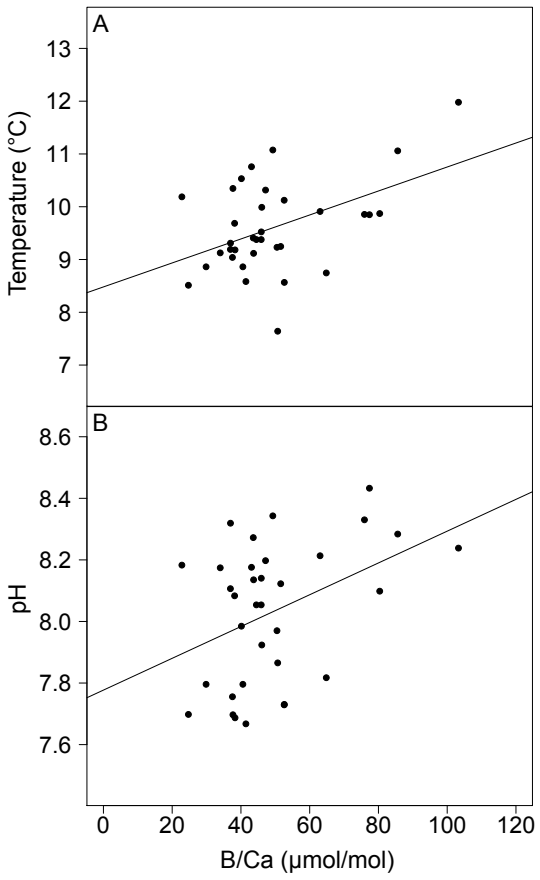

Fig. 8. (A) Relationship between *M. californianus* B/Ca from the inner prismatic layer and measured temperature (Adj. $R^2 = 0.189$, $p = 0.0059$). **(B)** Relationship between *M. californianus* B/Ca from the inner prismatic layer and measured pH (Adj. $R^2 = 0.135$, $p = 0.019$).

became low and no longer statistically significant. This result was consistent with the typical number of samples and width of the growth band, assuming a sinusoidal growth pattern.

3.3 Calculation of K_D

The partition coefficient, K_D, was calculated following Eq. (1). Estimated K_D was calculated for each sample point. Total dissolved inorganic carbon (DIC), total alkalinity (ALK) and anthropogenic CO_2 in surface waters were estimated by the CO2sys Excel Macro (Pierrot et al., 2006) using primarily data from the Hydrolab instrument (Wootton et al., 2008) and supplemented by the GLODAP hydrographic dataset (Key et al., 2004). The $K_D \times 1000$ values for all samples ranged from 0.83 to 2.84 (Fig. 9).

4 Discussion

4.1 Environmental control on B/Ca

To assess the feasibility of using B/Ca in mussels as an indicator of ocean pH, B/Ca data derived from our *M. californianus* specimen are compared to the 9-year record of environmental data from the same location. Because instrumental data is available only from the summer months due to logistic constraints, correlation is calculated only at times where concurrent data points exist between the two datasets. As described in the section on growth chronology, both pH and temperature provided the highest correlation between environmental data and B/Ca data as compared to other environmental parameters such as atmospheric CO_2, chlorophyll-*a*, estimated alkalinity, salinity, daily upwelling index, and PDO index. Our best-fit growth models provide the maximum possible fit between these two datasets, which is an r^2 of 0.207 for pH and 0.256 for temperature-based on data from all three calcitic shell layers (Fig. 3). Using data only from the longest transect from the inner prismatic layer of the shell, maximum r^2 values with the best-fit model of 0.256 ($p = 0.0031$) and 0.192 ($p = 0.018$) are obtained for pH and temperature, respectively. While these correlations are statistically significant, they are not sufficiently robust to use shell B/Ca as a proxy for seawater pH, particularly considering that B/Ca and temperature exhibits a stronger relationship (Fig. 8). Additionally, correlations between shell B/Ca and temperature and pH vary based on environmental bin size even within the best-fit model. For example, the coefficient of determination between shell B/Ca and temperature varies from 0.256 with a significant p-value of 0.0031 at a 5-day bin size to an r^2 of 0.065 with a non-significant p-value of 0.123 using a 13-day bin size. We also find large variation between growth patterns among years. For example, the best-fit model analysed on within-year data yields poor r^2 values of 0.120

and 0.180 in 2004, yet higher r^2 values of 0.265 and 0.967 in 2005 for pH and temperature, respectively. Thus, we see at best an r^2 of 0.256 between the B/Ca data and any environmental variable, in this case temperature. This variation highlights the importance of understanding temporal patterns of organismal growth and calcification to the interpretation of geochemical proxy data. Based on this relatively poor best-fit correlation and high variation in within-year correlations between B/Ca and pH and temperature, we conclude that other factors, likely vital effects, are contributing strongly to B incorporation in *M. californianus*. In the following sections we explore the controls on B/Ca in the bivalve shell beyond pH or temperature.

4.2 Physiological control

4.2.1 Winter bands

The most distinct features of the B/Ca data are the peaks corresponding with winter bands observed in the inner prismatic layer record. Because of the patterns of shell accretion in *M. californianus*, the winter bands tend to have a net accumulation of organic matter relative to the thick bands deposited during summer growth; a particularly long or severe winter prolongs the period of slow growth and potential shell dissolution due to low metabolic rates, and thereby contributes to an increase in excess organic matter left behind from carbonate dissolution in the winter band (Lutz and Rhoads, 1977; Takesue et al., 2008). Our data reveal particularly high B/Ca excursions during the winters of 2004–2005 and 2005–2006. The spring transition (i.e. initiation of upwelling) in 2005 was delayed by 50 days from the long-term mean (NOAA Fisheries, www.nmfs.noaa.gov), which may be associated with a phenological delay in 2005 and 2006. This evidence for prolonged winter climate conditions is consistent with the best sample chronologies found in our study, which are associated with sinusoidal, temperature-dependent growth. A delay in the onset of faster shell accretion means that the mussel experiences a longer period of slow or nonexistent net growth at low temperatures.

4.2.2 Calcification

The B/Ca compositions of the three different growth layers are not identical as would be predicted if they were controlled only by external environmental parameters (Fig. 6). Average B/Ca values for the beak, inner prismatic, and outer prismatic are 66, 45, and 39 µmol mol^{-1}, respectively. The differences in the measurements from these layers may be attributed in part to differences in the sampling resolution, and also to differences in the growth pattern. The difference in the distance between growth checks in each of the layers may cause higher resolution sampling in some layers and some years versus others. For example, the outer prismatic layer extends farther in diameter around the outside of the shell than does the inner prismatic layer. However, this outer layer may be differentially eroded by its greater exposure to the external environment. It thus provides a less complete record than the inner layers and as such is not useful for evaluating the B/Ca proxy.

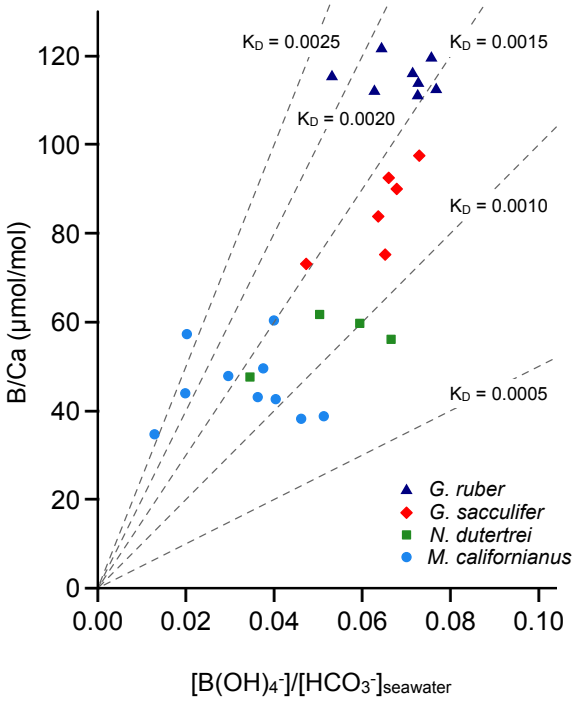

Fig. 9. *M. californianus* B/Ca from the inner prismatic layer 2000–2009 in blue circles plotted with planktonic foraminiferal B/Ca from Foster (2008): *N. dutertrei* in green squares, *G. sacculifer* in red diamonds, and *G. ruber* in navy triangles.

B/Ca in the beak region is systematically higher than those in the inner and outer prismatic layers (46 % higher than the inner prismatic and 69 % higher than the outer prismatic). As with B/Ca excursions present in winter bands, this offset can in part be attributed to accumulation of organic matter in this part of the shell, suggested by the dark brown colour of the shell material (Takesue et al., 2008). A recent study by Takesue et al. (2008) showed a 33 % average decrease in Mg/Ca, 78 % average decrease in Mn/Ca, and 0–36 % decrease in Ba/Ca in *Corbula amurensis*, the Asian clam, after removal of organic matter using an oxidative cleaning procedure. This mechanism is consistent with higher mean measured B/Ca in the organic-rich beak region than in the other shell layers.

The differences in B/Ca between layers, and the lack of strong correlation between pH and B/Ca indicates that the bivalve exerts a strong physiological control on its shell chemistry. Details of B incorporation into biogenic carbonates and relationships between B/Ca and δ^{11}B are not well defined, even in foraminifera and corals, which have been examined most closely (Allison et al., 2010; Pagani et al., 2005).

Despite this uncertainty, it is clear that most calcifying organisms precipitate carbonate material from an extracellular calcifying fluid from within the organism (see Allison et al., 2010; Meibom et al., 2008, for details in corals; Griffith et al., 2008, for forams; Klein et al., 1996; Takesue et al., 2008; Weiner and Dove, 2003, for bivalves), and that many organisms alter the chemical composition and pH of this extracellular fluid (Rollion-Bard et al., 2011a, b; Klein et al., 1996; Weiner and Dove, 2003).

Focus on development of the B/Ca and δ^{11}B proxies has largely been on foraminifera and corals. However, studies of several trace elements in bivalves (occasionally including B) can provide useful insights. In general, high levels of trace elements in biogenic carbonates have been related to elevated organic matter concentrations (Lutz and Rhoads, 1977; Takesue et al., 2008). However, elevated trace element abundances in bivalves may also be related to higher growth rates resulting from greater calcification rates (Takesue et al., 2008). In aragonitic bivalves, faster crystal growth rates are associated with higher trace element enrichment because Ca-channels that transport ions through the calcification mantle become less ion-selective when Ca^{2+} fluxes are higher to support faster crystal growth (Carré et al., 2006). Other data from *Mytilus edulis* show that trace element incorporation may increase with mussel filtration rates, which may also be indicative of higher trace element abundances associated with faster growth, albeit by a different mechanism (Phillips, 1976; Janssen and Scholtz, 1979). Furthermore, Takesue et al. (2008) report trace element enrichment in the larger of two asymmetrical valves of the same individual of the aragonitic bivalve *C. amurensis*. It must again be noted that B incorporation is thought to be primarily via $B(OH)_4^-$ competition with CO_3^{2-} and not Ca^{2+} (Hemming and Hanson, 1992), and it is not well understood how similar mechanisms of cation vs. anion transport operate (Allison et al., 2010) or how much incorporation of $B(OH)_3$ contributes to the presence of B in the shell (Rollion-Bard et al., 2011a). Thus, we stress the importance of testing B incorporation in different species and in different environments to explore biological mechanisms of incorporation.

Differences between predicted pH from B/Ca and what has been measured in situ must be caused by physiological factors. The shell of *M. californianus* is secreted by the mantle, which precipitates calcium carbonate from the extrapallial fluid within it. There are two possible mechanisms for the passage of calcium and other ions across the epithelial layer into the extrapallial fluid, intercellular or intracellular, though intracellular transport is expected to be more Ca-specific (Klein et al., 1996). Through these mechanisms, which are not yet well-described (Klein et al., 1996; Takesue et al., 2008), *M. californianus* may exert biological control through ion transport mechanisms or other metabolic effects on the trace element concentration and pH of its extrapallial fluid, causing the chemical composition of its shell to reflect values other than those of ambient seawater (Klein et al., 1996) and thus compromising the ability of the B system to predict pH (Reynaud et al., 2004). In general, maintenance of carbonate ion saturation at the calcification site is associated with elevation of pH and alkalinity within the calcifying fluid (Weiner and Dove, 2003), which can confound the chemical signatures of ambient seawater. In a recent paper, Rollion-Bard et al. (2011b) find a similarly variable relationship between δ^{11}B and known pH values (in their case, constant pH) at the site of growth in the corals *Cladocora caespitosa* and *Porites lutea*. It is thus important to note that significant vital effects may also be problematic in species that are considered to be well understood relative to bivalves.

By contrast, relationships have been described between B/Ca and both carbon chemistry and temperature on the species level in planktonic foraminifera (Foster, 2008; Yu et al., 2007). We explored whether the large-scale variations in seawater chemistry observed in these studies could be responsible for the observed relationships. For example, in a 2008 study by Foster, core-top samples of three species of Caribbean planktonic foraminifera, *G. ruber, G. sacculifer*, and *N. dutertrei*, were analysed for B/Ca (Fig. 9). Among habitats, $[CO_2]$ varied between roughly 130–330 µmol kg^{-1}, temperature varied from 19–30 °C, $[B(OH)_4^-]/HCO_3^-]$ ranged 0.047–0.077, and B/Ca varied from 80–130 µmol mol^{-1}. This led to a variation in $K_D \times 1000$ of 0.85–2.17 over three species. In contrast, $[CO_2]$ varied between roughly 64–210 µmol kg^{-1}, yearly average temperature 9–11 °C, and yearly average B/Ca 34–60 µmol mol^{-1} over 10 years in our study (refer to Sects. 2.5 and 3.3 for details on our calculations of K_D). Despite these comparatively small environmental variations, including a $[B(OH)_4^-]/HCO_3^-]$ range from 0.012–0.051, our samples still yield larger variation in $K_D \times 1000$ (0.83–2.84) than observed in foraminifera studies. In other words, we see a smaller variation in $[CO_2]$, temperature, and B/Ca and yet a comparable variation in $[B(OH)_4^-]/HCO_3^-]$ and K_D in one bivalve species, *M. californianus* compared to the total range of B/Ca responses to those parameters in three different planktonic foraminifera species *G. ruber, G. sacculifer*, and *N. dutertrei* (Fig. 9). This means that a large variation in seawater carbonate chemistry has only a small effect on the shell chemistry of *M. californianus* when compared to foraminifera, who exhibit large changes in their shell B/Ca in response to small changes in seawater carbonate chemistry (i.e. foraminifera are more sensitive to changes in carbonate chemistry). This argues for strong physiological control over B incorporation in *M. californianus*, as the organism must strongly control its chemical environment in order to show such small variation in B/Ca over a relatively large range of $[B(OH)_4^-]/HCO_3^-]$.

When we compare the *M. californianus* record to individual species of foraminifera, we see that *G. ruber* and *N. dutertrei* exhibit a similar pattern but at a lower magnitude than *M. californianus* (e.g. a positive trend with large

spread over $[B(OH)_4^-)/HCO_3^-]$ and small spread over B/Ca), while *G. sacculifer* data show a different pattern (e.g. a positive trend with a small spread over $[B(OH)_4^-)/HCO_3^-]$ and a large spread over B/Ca), although the absolute variance of *M. californianus* over both axes much exceeds that of any foraminiferal species. In summary, the physiological control exerted by *M. californianus* is stronger than observed species-specific effects in foraminifera. Furthermore, B/Ca appears more correlated with temperature than with carbon chemistry in foraminifera (Foster, 2008; Yu et al., 2007), a pattern repeated in our analysis of *M. californianus* (Fig. 8). Whether this relationship is caused by increased growth rates at higher water temperatures or due to kinetic effects on K_D (Eqs. 1–3) remains unclear.

5 Conclusions

Assigning a within-year sample chronology to sclerochronological data can lead to uncertainty between environmental variation and contemporaneous organism growth, particularly when growth rates may vary from year to year or within a season. This study not only provides a framework to deal with such uncertainties where environmental and geochemical data are available at high resolution, but also highlights the importance of differential assumptions about organismal growth on the relationship between skeletal chemistry and environmental variation. While it appears from these results that both pH and temperature play a role in controlling the incorporation of B in the shells of *M. californianus*, and statistically significant relationships between shell B/Ca and both temperature and pH are established, we nevertheless conclude that B/Ca in an accretionary bivalve does not provide the strong relationship between shell chemistry and the seawater environment that is necessary for a reliable geochemical proxy. Instead, we find biological control to be an important mechanism on shell B/Ca chemistry, presumably through control of the internal calcifying fluid. This result is surprising considering the clear relationships that have been found between seawater chemistry, B/Ca and $\delta^{11}B$ in many other species. Further work investigating the role of both substitution chemistry and physiological control on B/Ca and $\delta^{11}B$ may help to explain the discrepancy between the roles played by pH in controlling each of these proxies.

Acknowledgements. Financial support was provided by USGS-WHOI Co-operative agreement and NSF-ANT award number 0902957 to L. F. Robinson, a SeaDoc Society grant to C. A. Pfister and J. T. Wootton, and a NASA Planetary Biology Internship to S. J. McCoy with L. F. Robinson and D. M. Glover. The authors would like to thank M. Auro for technical assistance, and D. M. Glover, A. Kandur, and D. A. Kennedy for computational and statistical advice.

Edited by: A. Shemesh

References

Al-Ammar A., Gupta R. K., and Barnes, R. M.: Elimination of boron memory effect in inductively coupled mass spectrometry by addition of ammonia, Spectrochimica Acta, Part B, 54, 1077–1084, 1999.

Al-Ammar, A., Reitznerova, E., and Barnes, R. M.: Improving boron isotope ratio measurement precision with quadrupole inductively copuled plasma-mass spectrometry, Spectrochimica Acta, Part B, 55, 1861–1867, 2000.

Allison, N., Finch, A. A., and EIMF.: $\delta^{11}B$, Sr, Mg and B in a modern *Porites* coral: the relationship between calcification site pH and skeletal chemistry, Geochim. Cosmochim. Acta, 74, 1790–1800, doi:10.1016/j.gca.2009.12.030, 2010.

Blamart, D., Rollion-Bard, C., Cuif, J.-P., Juillet-Leclerc, A., and Dauphin, Y.: Correlation of boron isotopic composition with ultrastructure in the deep-sea coral *Lophelia pertusa*: Implications for biomineralization and paleo-pH, Geochem. Geophys. Geosys., 8, Q12001, doi:10.1029/2007GC001686, 2007.

Broecker, W. S. and Peng, T.-H.: Tracers in the Sea, Eldigo Press, Palisades, New York, USA, 690 pp., 1982.

Caldeira, K. and Wickett, M. E.: Anthropogenic carbon and ocean pH, Nature, 425, 365–365, 2003.

Carré, M., Bentaleb, I., Bruguier, O., Ordinola, E., Barrett, N. T., and Fontugne, M.: Calcification rate influence on trace element concentrations in aragonitic bivalve shells: evidences and mechanisms, Geochim. Cosmochim. Acta, 70, 4906–4920, 2006.

Coe, W. R.: Nutrition and growth of the California Bay-Mussel (*Mtilus edulis diegensis*), J. Exp. Zool., 99, 1–14, 1965.

Dodd, J. R.: Environmentally controlled variation in the shell structure of a pelecypod species, J. Paleontology, 38, 1065–1071, 1964.

Foster, G. L.: Seawater pH, pCO_2 and $[CO_3^{2-}]$ variation in the Caribbean Sea over the last 130 kyr: A boron isotope and B/Ca study of planktic foraminifera, Earth Planet. Sci. Lett., 271, 254–266, 2008.

Foster, L. C., Finch, A. A., Allison, N., Andersson, C., and Clarke, L. J.: Mg in aragonitic bivalve shells: Seasonal variations and mode of incorporation in *Arctica islandica*, Chemical Geology, 254, 113–119, 2008.

Goodwin, D. H., Flessa, K. W., Schöne, B. R., and Dettman, D. L.: Cross-calibration of daily growth increments, stable isotope variation, and temperature in the Gulf of California bivalve mollusk *Chione cortezi*: Implications for paleoenvironmental analysis, Palaios, 16, 387–398, 2001.

Griffith, E. M., Paytan, A., Kozdon, R., Eisenhauer, A., and Ravelo, A. C.: Influences on the fractionation of calcium isotopes in planktonic foraminifera, Earth Planet. Sci. Lett., 268, 124–136, 2008.

Hart, S. R. and Cohen, A. L.: An ion probe study of annual cycles of Sr/Ca and other trace elements in corals, Geochim. Cosmochim. Acta, 60, 3075–3084, 1996.

Hemming, N. G. and Hanson, G. N.: Boron isotopic composition and concentration in modern marine carbonates, Geochim. Cosmochim. Acta, 56, 537–543, 1992.

Hönisch, B. and Hemming, N. G.: Surface ocean pH response to variations in pCO_2 through two full glacial cycles, Earth Planet. Sci. Lett., 236, 305–314, 2005.

Hönisch, B., Hemming, N. G., and Loose, B.: Comment on "A critical evaluation of the boron isotope-pH proxy: The accuracy

of ancient ocean pH estimates" by M. Pagani, D. Lemarchand, A. Spivack and J. Gaillardet, Geochim. Cosmochim. Acta, 71, 1636–1641, 2007.

Janssen, H. H. and Scholtz, N.: Uptake and cellular distribution of cadmium in *Mytilus edulis*, Mar. Biol., 55, 133–141, 1979.

Kennish, M. J. (Ed.): Chapter 2: Marine Chemistry: 45–53, CRC Practical Handbook of Marine Science, CRC Press, Inc., Boca Raton, FL, USA, 1989.

Key, R. M., Kozyr, A., Sabine, C. L., Lee, K., Wanninkhof, R., Bullister, J. L., Feely, R. A., Millero, R. F., Mordy, C., and Peng, T. H.: A global ocean carbon climatology: Results from Global Data Analysis Project (GLODAP), Global Biogeochem. Cycles, 18, GB4031, doi:10.1029/2004GB002247, 2004.

Killingly, J. S. and Berger, W. H.: Stable isotopes in a mollusk shell: Detection of upwelling events, Science, 205, 186–187, 1979.

Klein, R. T., Lohman, K. C., and Thayer, C. W.: Sr/Ca and $^{(}13)C/^{(}12)C$ ratios in skeletal calcite of *Mytilus trossulus*: Covariation with metabolic rate, salinity, and carbon isotopic composition of seawater, Geochim. Cosmochim. Acta, 60, 4207–4221, 1996.

Klochko, K., Cody, G. D., Tossell, J. A., Dera, P., and Kaufman, A. J.: Re-evaluating boron speciation in biogenic calcite and aragonite using δ^{11}B MAS NMR, Geochim. Cosmochim. Acta, 73, 1890–1900, 2009.

Lee, K., Kim, T.-W., Byrne, R. H., Millero, F. J., Feely, R. A., and Liu, Y.-M.: The universal ratio of boron to chlorinity for the North Pacific and North Atlantic oceans, Geochim. Cosmochim. Acta, 74, 1801–1811, 2010.

Lemarchand, D., Gaillardet, J., Lewin, E., and Allegre, C. J.: The influence of rivers on marine boron isotopes and implications for reconstructing past ocean pH, Nature, 408, 951–954, 2000.

Lutz, R. A.: Electron probe analysis of strontium in mussel (Bivalvia, Mytilidae) shells: Feasibility of estimating water temperature, Hydrobiologia, 83, 377–382, 1981.

Lutz, R. A. and Rhoads, D. C.: Anaerobiosis and a theory of growth line formation, Science, 198, 1222–1227, 1977.

Malone, P. G. and Dodd, J. R.: Temperature and salinity effects on calcification rate in *Mytilus edulis* and its paleoecological implications, Limnol. Oceanogr., 12, 432–436, 1967.

Meibom, A., Cuif, J.-P., Houlbreque, F., Mostefaoui, S., Dauphin, Y., Meibom, K. L., and Dunbar, R.: Compositional variations at ultra-structure length scales in coral skeleton, Geochim. Cosmochim. Acta, 72, 1555–1569, 2008.

Pagani, M., Lemarchand, D., Spivack, A., and Gaillardet, J.: A critical evaluation of the boron isotope-pH proxy: The accuracy of ancient ocean pH estimates, Geochim. Cosmochim. Acta, 69, 953–961, 2005.

Paine, R. T. and Trimble, A. C.: Abrupt community change on a rocky shore – biological mechanisms contributing to the potential formation of an alternative state, Ecol. Lett., 7, 441–445, 2004.

Pfister, C. A., Wootton, J. T., and Neufeld, C. J.: Relative roles of coastal and oceanic processes in determining physical and chemical characteristics of an intensively sampled nearshore system, Limnol. Oceanogr., 52, 1767–1775, 2007.

Phillips, D. J. H.: The common mussel *Mytilus edulis* as an indicator of polluiton by zinc, cadmium, lead and copper. I: Effects of environmental variables on the uptake of metals, Mar. Biol., 38, 59–69, 1976.

Pierrot, D., Lewis, E., and Wallace, D. W. R.: CO2sys DOS program developed for CO2 system calculations. ORNL/ CDIAC-105. Carbon Dioxide Information Analysis Center, Oak Ridge National Laboratory, US Department of Energy, Oak Ridge, TN, 2006.

Reynaud, S., Hemming, N. G., Juillet-Leclerc, A., and Gattuso, J. P.: Effect of pCO_2 and temperature on the boron isotopic composition of the zooxanthellate coral *Acropora* sp., Coral Reefs, 23, 539–546, 2004.

Rollion-Bard, C., Blamart, D., Trebosc, J., Tricot, G., Mussi, A., and Cuif, J.-P.: Boron isotopes as pH proxy: a new look at boron speciation in deep-sea corals using ^{11}B MAS NMR and EELS, Geochim. Cosmochim. Acta, 75, 1003–1012, 2011a.

Rollion-Bard, C., Chaussidon, M., and France-Lanord, C.: Biological control of internal pH in scleractinian corals: Implications on paleo-pH and paleo-temperature reconstructions, C. R. Geoscience, 343, 397–405, 2011b.

Sah, R. N. and Brown, P. H.: Boron determination: A review of analytical methods, Microchem. Journ., 56, 285–304, 1997.

Sanyal, A., Nugent, M., Reeder, R. J., and Buma, J.: Seawter pH control on the boron isotopic composition of calcite: Evidence from inorganic calcite precipitation experiments, Geochim. Cosmochim. Acta, 64, 1551–1555, 2000.

Schöne, B. R., Rodland, D. L., Fiebig, J., Oschmann, W., Goodwin, D., Flessa, K. W., and Dettman, D.: Daily growth rates in shells of *Arctica islandica*: Assessing sub-seasonal environmental controls on a long-lived bivalve mollusk, Palaios, 20, 78–92, 2005.

Schöne, B. R., Houk, S. D., Castro, A. E. F., Fiebig, J., Oschmann, W., Kroncke, I., Dreyer, W., and Gosselck, F.: Reliability of multitiaxon, multiproxy reconstructions of environmental conditions from accretionary biogenic skeletons, J. Geol., 114, 267–285, 2006.

Sen, S., Stebbins, J. F., Hemming, N. G., and Ghosh, B.: Coordination environments of boron impurities in calcite and aragonite polymorphs: an ^{1}1B MAS NMR study, Am. Mineral, 79, 818–825, 1994.

Shimizu, N. and Hart, S. R.: Applications of the ion microprobe to geochemistry and cosmochemistry, Ann. Rev. Earth Planet. Sci., 10, 483–526, 1982.

Spivack, A. J. and Edmond, J. M.: Boron isotope exchange between seawater and the oceanic crust, Geochim. Cosmochim. Acta, 51, 1033–1043, 1987.

Stoll, H., Shimizu, N., Arevalos, A., Matell, N., Banasiak, A., and Zeren, S.: Insights on coccolith chemistry from a new ion probe method for analysis of individually picked coccoliths, Geochem. Geophys. Geosys., 8, Q06020, doi:10.1029/2006GC001546, 2007.

Takesue, R. K. and van Geen, A.: Mg/Ca, Sr/Ca and stable isotopes in modern and Holocene *Protothaca staminea* shells from a northern California coastal upwelling region, Geochim. Cosmochim. Acta, 8, 3845–3861, 2004.

Takesue, R. K., Bacon, C. R., and Thompson, J. K.: Influences of organic matter and calcification rate on trace elements in aragonitic estuarine bivalve shells, Geochim. Cosmochim. Acta, 72, 5431–5445, 2008.

Weiner, S. and Dove, P. M.: An overview of biomineralization processes and the problem vital effect, Rev. Mineral. Geochem., 54, 1–29, 2003.

Wootton, J. T., Pfister, C. A., and Forester, J. D.: Dynamic pat-

terns and ecological impacts of declining ocean pH in a high-resolution multi-year dataset, Proc. Natl. Acad. Sci., 105, 18848–18853, 2008.

Yu, J. and Elderfield, H.: Benthic foraminiferal B/Ca ratios reflect deep water carbonate saturation state, Earth Planet. Sci. Lett., 258, 73–86, 2007.

Yu, J., Elderfield, H., and Hönisch, B.: Tropical sea-surface temperature reconstruction for the early Paleogene using Mg/Ca ratios of planktonic foraminifera, Paleoceanography, 22, PA2202, doi:10.1029/2006PA001347, 2007.